A High-Accuracy Alignment System Based on the Dispersion Effect

H. Ingensand, B. Boeckem
Institute for Geodesy and Photogrammetry, ETH Zurich, Switzerland

1. INTRODUCTION

All geodetic systems utilizing electromagnetic waves in the visible or near IR-range must take the characteristics of the medium into account in which propagation occurs. As more sophisticated electro-optical systems for precision measurements are developed, more details of the propagation medium and coevally solutions of atmospherically induced limitations will become important.

Density variations in this propagation medium, i.e. in the air, due to spatial and temporal variations in the atmospheric states, e.g. temperature and pressure, cause inhomogeneities in the refractive index field which lead to gradients in the refractive index of the air. Considering laboratory conditions the detrimental influences of the ambient air arise in the quasi-stationary gradients which appear to have a large systematic component. These refraction effects induce discrepancies in angle between the true and the apparent direction, which are called the refraction angles [see Fig. 1].

Furthermore a contribution towards a turbulent atmosphere has to be made. In an indoor measurement scenario larger turbulent structures with a long-lasting influence can cause similar effects at low frequencies, as described above.

Hence the accuracy of the in-air alignment is not limited by the precision of the alignment systems but by these inhomogeneities in the atmosphere that cannot be averaged out within reasonable integration times [1].

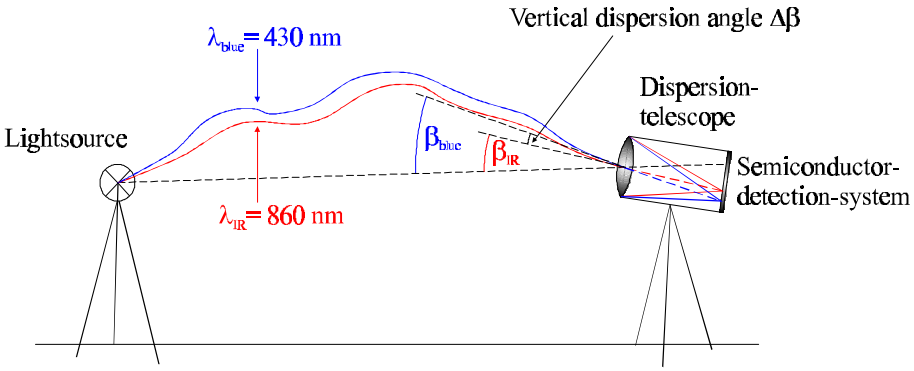

Fig. 1 Dispersometer principle for deriving the angle of refraction in a dispersive medium. The angles b_{blue} and b_{IR} depict the refraction angles for blue light and IR.

As a consequence a dispersometer for a metrological solution of atmospherically induced problems in high-accuracy optical alignment and direction observations is currently under construction at the Institute of Geodesy and Photogrammetry of the Swiss Federal Institute of Technology, Zurich (ETH). This design is capable of true, i.e. refraction compensated angle measurements, the detrimental influence of atmospheric turbulence notwithstanding, by using the two-color method in the dispersive air.
The principle of the two-color method utilizes the wavelength dependence of the refractive index. The difference angle between two light beams of different colors is to first approximation proportional to the refraction angle. Therefore, correcting the apparent direction by the refraction angle one will get the refraction free direction, in terms of alignment tasks the desired straight line [see Fig. 1]. However, the required accuracy can only be achieved by compensating the effects of atmospheric turbulence. In the currently developed dispersometer the same system will be capable of compensating both effects.
[2] is credited for the original idea of using the dispersion on angular measurements. For the last decades a large amount of research and development has been raised, but gaining inconclusive results. Feasibility in applying the dispersion effect in context with an alignment system has been shown by [1]. The ETH-dispersometer can be regarded as a further development of the WILD dispersometer subsystem of the Rapid Precision Leveling System (RPLS) [3], [4], [5] using the same detection optics (dispersion telescope) and a similar concept.
The major difficulties in instrumental realization arise in the availability of a suitable two-color light source and a high resolution semiconductor detection system and lacking in an appropriate turbulence compensation mechanism, not to mention the instrumental designs of the last decades, see [6], [7], [8] for an overview.

2. THEORY

In this section a presentation of the essential theory related to the dispersometer concept will be given.

2.1 Light propagation through the atmosphere

The light propagation as the propagation of an electromagnetic wave through the atmosphere is described by the MAXWELL equations. For a purely monochromatic wave, e.g. single mode laser radiation, in an isotropic inhomogenous medium the following second-order wave equation for the electric field vector **E** results:

$$\nabla^2\mathbf{E} + k^2 n^2 \mathbf{E} + 2\nabla\left[\mathbf{E}\cdot\nabla\, log(n)\right] = 0 \qquad (1)$$

where k is the wave number of the radiation and n depicts the local value of the refractive index of the medium, e.g. air. Assuming no depolarization in propagation [9] one can neglect the third term in (1):

$$\nabla^2\mathbf{E} + k^2 n^2 \mathbf{E} = 0 \qquad (2)$$

Due to random n an exact solution is generally not possible. (2) is called the Helmholtz equation which is the basis of the analysis by [1] for the complex amplitude of a component of the electric

field. Applying the geometrical optics approach by neglecting the finiteness of the wavelength, one can derive the eikonal equation [10], a relation between the refractive index n in a point, e.g. receiver, and the optical path length $\bar{s}$ between an origin, e.g. the light source, and that point [11]

$$(\nabla \bar{s})^2 = n^2 \tag{3}$$

where $\bar{s}$ is a scalar function of position. (3) is related to the FERMAT´s principle. An unified theory of angular refraction is presented by [12] on the basis of a solution of the eikonal equation by means of expansion by power series. From this analysis follows that the refraction angle in horizontal direction and the vertical refraction angle as functions of the refractive index and its partial derivatives can be described by

$$\alpha = \frac{1}{s \cdot \cos\beta} \int_0^s \frac{\partial n}{\partial Y} \, X \, dX \tag{4}$$

$$\beta = -\frac{1}{s} \int_0^s \frac{\partial n}{\partial Z} \, X \, dX \tag{5}$$

taking only first order terms into account. Wherein α is the horizontal and β the vertical component of the refraction angle, s the distance between light source and receiving unit along the X-axis. The introduced coordinate system can be exemplified in Fig. 1. The X-axis is oriented in direction light source - receiving unit. The Z-axis represents the vertical axis. In this paper the theory by [12] is accepted. The procedures presented by [1] are equivalent to the geometrical optics approach.

2.2 Dispersometer principle

The index of refraction can be expressed as the product of two terms:

$$n - 1 = \mu(\omega) \, F(x,y,z) \tag{6}$$

where the first factor μ depends on the frequency of radiation, i.e. on the wavelength used. It remains constant for a selected light source emitting a certain wavelength. F is a function of the density distribution of the propagation medium. The wavelength dependence of the refractive index is called dispersion, whereas air is a dispersive medium. The spatial dependence can be written in terms of the atmospheric states. Therefore (6) writes

$$n - 1 = \mu_1(\lambda) \, f_1(p,T) + \mu_2(\lambda) \, f_2(e,T) \tag{7}$$

wherein μ_1 and μ_2 are the dispersive terms and f_1, f_2 depending on the local temperature T, the pressure of the air p and the water vapor pressure e. For dry air (e = 0) the second term on the right hand side of (7) vanishes. Introducing (7) one can find for, e.g. the vertical refraction angle (5)

$$\beta = -\frac{\mu_1}{s} \int_0^s \frac{\partial f_1}{\partial Z} \, X \, dX - \frac{\mu_2}{s} \int_0^s \frac{\partial f_2}{\partial Z} \, X \, dX . \tag{8}$$

Setting up (8) for both wavelength the vertical dispersion angle writes

$$\begin{aligned}\beta_{blue} - \beta_{IR} = &-\frac{m_1(\lambda_{blue})}{s}\int_0^s \frac{\partial f_1}{\partial Z}\, X\, dX - \frac{m_2(\lambda_{blue})}{s}\int_0^s \frac{\partial f_2}{\partial Z}\, X\, dX \\ &+\frac{m_1(\lambda_{IR})}{s}\int_0^s \frac{\partial f_1}{\partial Z}\, X\, dX + \frac{m_2(\lambda_{IR})}{s}\int_0^s \frac{\partial f_2}{\partial Z}\, X\, dX\end{aligned} \tag{9}$$

wherein the first integral on the right hand side can be expressed by

$$-\frac{1}{s}\int_0^s \frac{\partial f_1}{\partial Z}\, X\, dX = \beta_{blue}\,\frac{1}{m_1(\lambda_{blue})} + \frac{m_2(\lambda_{blue})}{m_1(\lambda_{blue})}\,\frac{1}{s}\int_0^s \frac{\partial f_2}{\partial Z}\, X\, dX. \tag{10}$$

Inserting (10) into (9) and neglecting the second terms respectively which represent the correction due to water vapor, one finds the relation between the observed dispersion angle and the refraction angles for dry air in a representation related to the blue light refraction angle

$$\beta_{blue} = \frac{m_1(\lambda_{blue})}{m_1(\lambda_{blue}) - m_1(\lambda_{IR})}\,(\beta_{blue} - \beta_{IR}). \tag{11}$$

Regarding that the first factor on the right hand side of (11) represents a wavelength dependent constant, one can use the short form notation

$$\beta_{blue} = n\,(\beta_{blue} - \beta_{IR}) = n\,\Delta\beta. \tag{12}$$

Analogue results can be obtained for the calculation of the horizontal refraction angle. Exchanging the sign of the refraction integral in (5) the results given by [3], [1] in a slightly different analysis and representation can be obtained. The analysis shows that to this degree of approximation the refraction angles depend no longer on the atmospheric state conditions along the actual path. The wavelength dependent constant n, the reciprocal dispersive power [8] in accordance with [10], can be derived by laboratory measurements, e.g. using the dispersion formula by [13]. (11) and (12) imply that the dispersion angle has to be measured at least 43 times more accurate than the desired refraction angle for the wavelengths used in the ETH-dispersometer. Herein this required accuracy constitutes the major difficulty for the instrumental performance in applying the dispersion effect.

Equations (11) and (12) assume dry air (e = 0). For deviating ambient conditions a small humidity correction term has to be introduced. Theoretically the uncertainty due to the humidity term could be canceled by introducing a third wavelength [14], [6]. From a metrological point of view this approach is not feasible, because the resolution of the detection unit, which already reaches the technological limits, has to be increased by at least a factor of the order 10^2. However in case of an indoor alignment system the uncertainty due to water vapor gradients is not a critical issue. Considerations of the humidity contributed correction are given in the analysis of [6], [8], [11], [14], [15].

To describe the envisaged turbulence compensation in an indoor measurement situation, it seems to be favorable to discuss the turbulence structures in an heuristic way [16], [17]. Dividing the turbulent atmosphere into regions of varying refractive indices one will get a bubble-like structure of varying sizes and densities [3], [4]. Because of the aforementioned detrimental larger turbulent structures at low frequencies, which are expected to prevail in a laboratory environment, the ambient medium can be regarded as a lens-like medium. This signifies that a narrow beam will be tilted and deflected, rather than distorted, in terms of wavefront deformation, which appears to be similar to the effects due to quasi-stationary refractive index gradients. Therefore, the same scheme is able to compensate both effects [1], [3], [18].

However, the stochastic influences of atmospherical turbulence can be significantly reduced by extending integration time, which is possible using a semiconductor detection system. For further details see the simulations given in [3], [4].

For applying the two-color method the choice of the appropriate wavelength pairs plays an important role. Herein boundary values are determined by the two color theory, atmospheric propagation properties and by instrumental features, see section 3. Moreover the availability of a suitable dual-wavelength light source is the specifying factor.

In contradiction to the hitherto prevalent opinion, where the separation of the two wavelengths should be arranged as far as possible, a more detailed analysis has to be reviewed. An important assumption induced in the two wavelength theory is the necessity of the same optical paths for both wavelengths. The wider the spectral span and coevally the more this span is shifted towards the UV-range the larger is the amount of spatial separation for both beams. This implies on the one hand the wavelength dependent constant n decreases and the accuracy of determining the dispersion angle by constant resolution of the detection system increases. On the other hand a limit for the spectral separation due to the requirement of highly correlated beams with respect to variations of the refractive index along the path is introduced. As an expansion of the theory by [12], [14] and [19] consider the decorrelation of the two optical paths, but latter as an application of range correction. Furthermore details of transmission through the medium have to be taken into account. In the IR-range an atmospherically induced limitation is given by water vapor absorption. For this reason the longer wavelength must not coincide with an atmospheric absorption line. Towards the UV ozone absorption and atmospheric scattering increase [20]. Utilizing optical and electro-optical devices, their spectral range and sensitivity have to be taken into account for an optimum performance. For example using a single mode fiber to cut off high-order modes the frequency range is previously determined by the numerical aperture (NA) and the cut-off frequency, i.e. the shortest wavelength at which single mode propagation will occur within the fiber.

As mentioned above the most decisive value arises from the availability of the light source. Laser diodes, recommended because of their advantages of high efficiency, compact size, long lifetime and low cost, are available over a wide wavelength range from 630 nm to 2000 nm. Although a large amount has been put into research, and considerable improvements have been made, e.g. [21], it is still a long way for blue semiconductor lasers to become reliably operating devices [22]. An alternative compact laser source, which has the inherent dual-wavelength opportunity, is based on frequency conversion in bulk nonlinear crystals. Meeting the requirements for the phase matching conditions of a potassium niobate ($KNbO_3$) waveguide, the 860 nm for the fundamental wave and so the 430 nm for the second harmonic wave are a fairly optimized choice for a dispersometer.

The initial quantities of observation, the dispersion angles in the horizontal and vertical direction appear as the horizontal and vertical displacement components on the semiconductor detection

system in the focal plane of the dispersion telescope. Knowing the exact focal length f of the telescope one can calculate, e.g. the vertical dispersion angle $\Delta\beta$ with the relation given for a small angle

$$\Delta\beta = \frac{y_{blue} - y_{IR}}{f}. \qquad (13)$$

In (13) y_{blue} and y_{IR} are the displacement components in vertical direction assuming the y-axis of the detector coordinate-system is aligned to the Z-axis. And thereof using (12) finally, e.g. the vertical refraction angle β_{blue} for blue light can be obtained.

3. DESCRIPTION OF THE SYSTEM

In this report a state of the art dispersometer concept will be introduced as a further development of the RPLS dispersometer subsystem. Herein solutions for the most critical issues on the instrumental side, the suitable dual-wavelength light source and the high resolution semiconductor detection system, will be proposed and their envisaged performance discussed. Generally one can divide the dispersometer into two components, the light source, see subsection 3.1, and the detection unit, see subsection 3.2.

3.1 The ETH-dispersometer light source

The core of the ETH-dispersometer light source [see Fig. 2] is the dual-wavelength laser generating blue light by frequency doubling of a semiconductor laser diode in a bulky $KNbO_3$ waveguide [22]. For applying the dispersion effect a laser by second harmonic generation is ideally suited and leaves the problem of wavelength mixing.
The new developed laser generates 3.5 mW IR at 860.5 nm and 4.2 mW blue light at 430.25 nm. The decisive parameters, the wavelengths, have been measured with an accuracy of 0.1 nm at 860.5 nm. The output power was determined after passing the first dichroic beam splitter, as described below. A follow-up version will generate 10 mW blue light at 430.25 nm. The IR-portion (maximum value 500 mW) can be lowered to the same value. Further specifications are listed in (Table 1).

Wavelength	860.5 nm, 430.25 nm
Output power, cw	3.5 mW @ 860 nm, 4.2 mW @ 430 nm
Spatial mode	TEM_{00}
Beam quality, M^2	< 1.2 for blue light
Beam diameter, $1/e^2$ intensity	0.7 mm
Polarization	430 nm vertical, 860 nm horizontal
Operating temperature range	15 - 30 °C

Table 1 Specifications of the dual-wavelength laser

The limited temperature range can be expanded by introducing a more expendable cooling mechanism or shifted by optimizing the set-up for a different temperature range. The complete light source is installed in a box, noting the laser radiates 4 W of heat that has to be lead away.

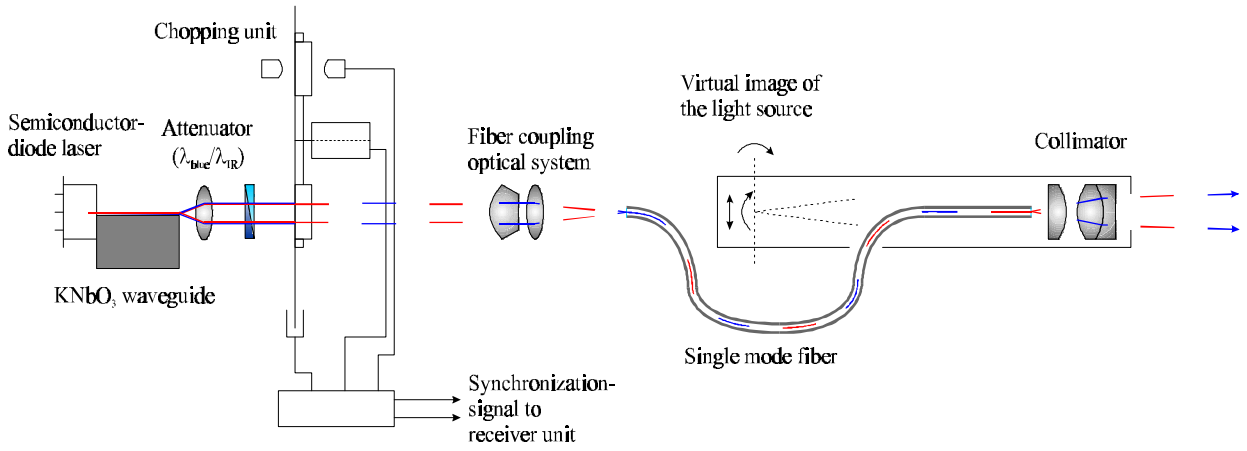

Fig. 2 Schematic drawing and realization of the ETH-dispersometer light source

The specifications of the dispersometer related to the detector electronics require a magnitude agreement of 1 % between the blue and the IR-radiant fluxes. To meet these requirements and also due to a non-ideal second harmonic generation efficiency, the power of the fundamental frequency has to be lowered. For coarse adjustment a dichroic beam splitter is mounted to the beam output. A second attenuator which is optical filter based will adjust both beams to equal intensity as a function of the path length because of propagation losses due to extinction, absorption and scattering. Furthermore it is proposed to replace the second attenuator by a dichroic beam splitter in order to significant less power losses by absorption as the one which is mounted to the laser.
Due to the detection scheme it is required to send the beams alternately. The correlation of the two optical paths demands a separation rather in time than in space. Therefore the chopping unit provides intensity modulation and wavelength selection as well. Wavelength selection is achieved by optical Schott glasses BG39 and RG780. With a thickness of the filter glasses of 4 mm a

blockage of more than 10^5 (40 dB) results, so that evidently no crosstalk between blue and IR occurs. Integrating the chopping unit into the light source will preserve several advantages. First of all vibrations due to a non-perfectly balanced chopper wheel will not effect the detection scheme. Another source of errors prevented is tilting of the filters in the filter wheel. By placing the chopping unit in front of the detector optics a small random tilt on each filter plate will produce a random displacement in the focal plane of the receiving optics [18]. The filter wheel with constant angular speed generates a temporal intensity modulation with a frequency of 250 Hz for each color. Herein the chopping frequency can be adjusted to the turbulent conditions, e.g. the turbulence frequency. In Fig. 3 the temporal intensity modulation for IR is depicted, the axis of abscissae dimension is in time per division, the axis of ordinates represents volt per division. This reference signal has been measured using an IR-light emitting diode and an appropriate photodiode directly on the filter wheel with a Tektronix THS 720 oscilloscope.

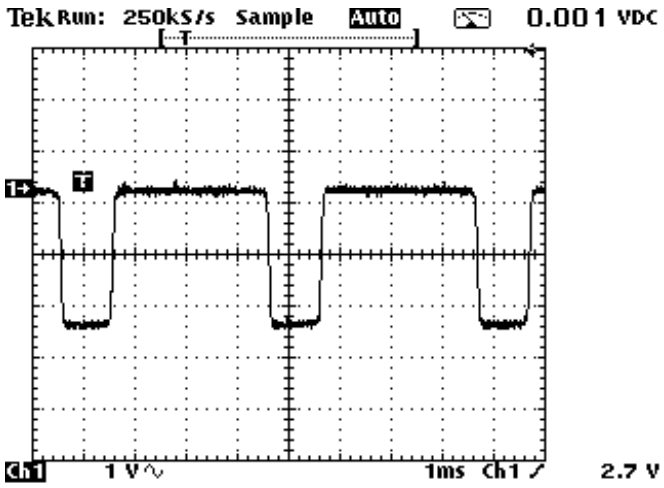

Fig. 3 The temporal intensity modulation for IR at a frequency of 250 Hz

The periods when neither blue nor IR are transmitted are used in the detection scheme for background and off-set measurements. For a color detection a reference signal via cable connection to the receiver unit is proposed. On a future stage an alternative synchronization scheme, e.g. by modulation of polarization, will be introduced.

After passing the filter wheel the two chopped beams are focused into a single mode fiber coupled by an optical fiber coupling system. Due to the introduced filter schemes both radiant fluxes are well adjusted. Therefore, an optimized coupling efficiency for both wavelengths will be precipitated. The single mode fiber, initially designed for an optimum coupling of the HeNe-laser radiation of 633 nm, with a cut-off wavelength of 420 nm, a core diameter of 2.5 µm and a cladding diameter of 130 µm, has been chosen to obtain a quasi-single mode propagation for both wavelength, i.e. to cut off high-order modes. A qualitative analysis of the beam image at the fiber end acknowledges single mode propagation and a good beam quality. To avoid detrimental backscattering that will make the semiconductor laser diode lase on different lines off the linewidth of the phase matching condition of the SHG-crystal, all optical components must not be aligned orthogonal to the incident beam. Therefore, a small angle of 7° is polished onto the fiber end. Besides homogenizing the laser beams using fiber optics will preserve several advantages, although launching in fibers is not possible without damping. The pointing of the sending optics is inde-

pendent of beam fluctuations and the size of the emitting optics is quite independent of the size of the light source. Furthermore the light source and the emitting optics are physically separated. Thus vibrations caused by the chopping unit will hardly effect the beam quality.
In the emitting scheme the same magnification for the two wavelengths is required to obtain one image plane for both colors. Otherwise a parallax would occur. Therefore, the emitting telescope at the fiber output consists of an achromatic well-corrected collector lens with a focal length of 8.8 mm. Moreover the essential requirement of coincidence of the centroids at both wavelengths can be met. In order to align the light source by moving in horizontal and vertical directions, the emitting telescope is mounted between the standards of an existing theodolite. The length of the telescope is calculated with the aim that the virtual images of the light source appear in the standing axis.

3.2 The receiving unit

After traveling along the optical path through the atmosphere both wavefronts are collected by an especially calculated dispersion telescope. The focal length of about 300 mm, by an assembly length of 260 mm, is determined by two boundary values. On the one hand this is the size of the detectable light spot blurred due to turbulence and on the other hand the detection accuracy which increases with increasing focal length (13) to a certain value limited by mechanical stability. Furthermore the dispersion telescope should not be much bigger than an ordinary theodolite telescope, planning to install both components in existing motorized theodolites. The ratio of the focal lengths for blue and IR is adjusted to dispersive conditions of a standard atmosphere. Therefore the same focal plane for both wavelengths can be obtained. With an additional lens combination one can adjust the appropriate dispersion of the optical system. The maximum entrance pupil of 75 mm can be reduced for experimental purpose, e.g. by analyzing the functional dependence of the turbulence compensation mechanism on the aperture size. The lens system is very precisely centered using wafer stepper objective technology by WILD [see Fig. 4].

Fig. 4 Dispersion telescope mounted on a WILD T2 theodolite,
additionally the dispersion telescope is rotatable around its optical axis.

Related to the theory proposed in section 2, the smallness of the wavelength dependent constant n implies that the dispersion angle has to be determined 42.6 times more accurate than the required refraction angle. Because of this reason the semiconductor detection system has to be capable of a resolution of better than 0.03 µrad assuming a refraction angle in the order of 1 µrad. This means a displacement resolution on the detector of approximately 10 nm by a predetermined focal length of 300 mm of the dispersion telescope. The semiconductor detection system is located in the focal plane of the dispersion telescope. In the ETH-dispersometer we are using a 4-quadrant position sensitive photodiode with an appropriate amplifier, which transforms the photocurrents induced in the quad-cell into electric potentials, to evaluate the blue- and IR spot displacements directly after the detector. Although the used position sensitive detector is a quad-cell photodiode type the quantum mechanical properties of the initially non-dotted small gap performing as a lateral detector are utilized [see Fig. 5].

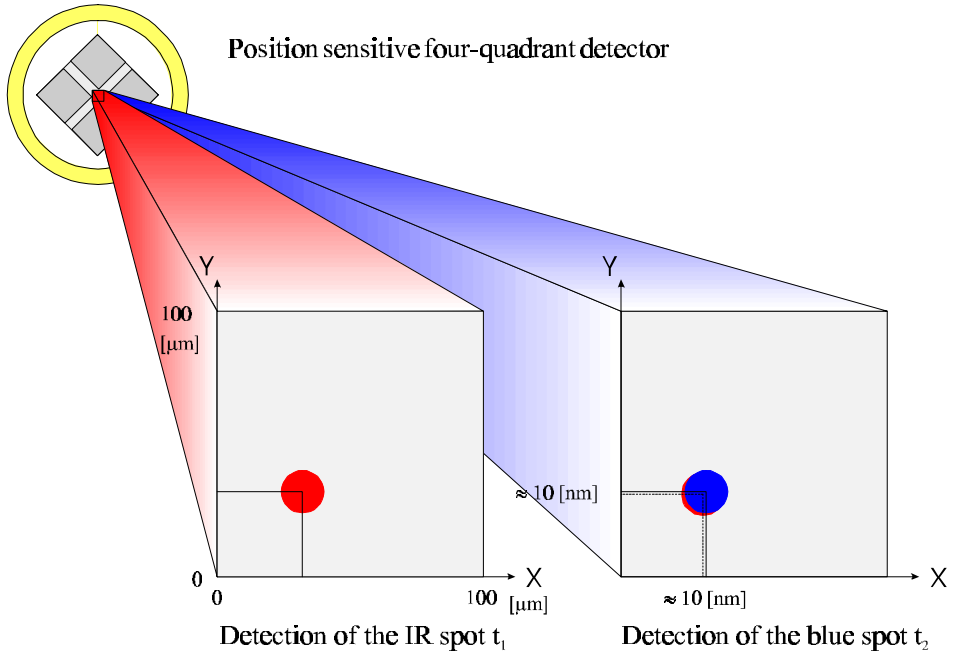

Fig. 5 Schematic drawing of the semiconductor detection scheme

Taking into account the dispersion of the telescope, due to not using a telescope of a Cassegrain-type, and the dispersion of the semiconductor-detection system as well a small correction can be computed. Furthermore an adjustment of the dispersion of the optics to that of the atmosphere is possible.

The ETH-dispersometer is one monolithic system. That means, with the exception of the wavelength dependent drifting and the wavelength dependent absorption depth on the photodiode, all impacts will affect both signals.

The data acquisition and processing system adapted to the emitting unit provides an in situ calculation of the dispersion angles, the pointing accuracy as a function of the integration time, power spectra of the dispersion angles and of the angle fluctuations at both wavelengths, the correlation between the two colors and the structure function of the refractive index derived from angle-of-arrival fluctuations [23].

4. APPLICATIONS AS A HIGH-ACCURACY ALIGNMENT SYSTEM

The feasibility study by [1] has shown that indoors discrepancies between true and apparent directions due to the ambient air can be reduced to less than 0.2 μrad using an integration time of 10 s. This means an alignment deviation of the refraction-corrected vertical direction to 4 μm at the distance of 20 m. Because the RPLS dispersometer subsystem has initially been designed for trigonometrical heights transfer, it has not been capable to deliver the horizontal and the vertical refraction angle simultaneously. With the use of a four-quadrant position sensitive photodiode in the ETH-dispersometer a two-dimensional refraction compensation is provided. This is highly required in high-accuracy alignment tasks. Assuming pointing towards the true direction, which represents the straight line to align to, slight deviations due to inhomogeneities in the field of the refractive index can be corrected by applying the proposed dispersometer principle. Refraction corrected optical alignment seems to be possible preserved by the fact that indoors no strong humidity gradients arise which cannot be compensated directly by applying the dispersion effect, otherwise correction terms have to be introduced.

5. CONCLUSION

Due to atmospherically induced limitations optical in-air alignment has not met the severe accuracy demands in connection with accelerator alignment [24]. One has either given up the applications of optical alignment systems or these systems have been installed in evacuated tubes. Furthermore the mechanical alignment systems are not influenced by the ambient air in terms of atmospherical refraction and turbulence, but will be affected by different impacts [24], [25]. Aside from this fact, the determination of vertical deviations by using a mechanical reference line underlies certain restrictions [25]. In respect of the highest accuracy requirements mechanical alignment systems will also be installed in at least closed tubes [24], [25].

With an alignment system based on the dispersion effect, as proposed in this paper, new possibilities in optical in-air alignment are given. Especially when one considers the fact that a dispersometer delivers refraction free direction integrally. That means evacuated tubes can be regarded as superfluous.

The ETH-dispersometer is designed to overcome the instrumental difficulties that arise in applying the two-color method, in an environment that is not affected by large humidity gradients, the concept works, especially for short and medium distanced sight lengths as given in the proposed projects. Encouraged by the results of [1], [3], [4] the size of the dispersometer can be small in contradiction to the previously prevalent opinion [26]. Therefore it is proposed to install both components in existing motorized theodolites. In the scope of the development of the ETH-dispersometer a comparison to the results, especially of [1] and reproduction of the former experiments is envisaged in order to gain further knowledge about light and IR-propagation through the atmosphere for geodetic applications.

6. REFERENCES

[1] A. M. J. Huiser, B. F. Gaechter, *A solution to atmospherically induced problems in very high-accuracy alignment and levelling*, in Applied Physics, 1989, Vol. 22, pages 1630-1638.

[2] E. Hertzsprung, *Photographische Messung der atmosphärischen Dispersion*, in Astron. Nachr., 1912, Vol. 192, pages 308-319.

[3] B. F. Gaechter, A. M. J. Huiser, *The Rapid Precision Levelling System Project*, Proceedings of IUGG (Vancouver), 1987, 20 pages.

[4] WILD LEITZ, *The development of a Rapid Precision Levelling System. Phase I: design specifications for a RPLS; performed under contract to the United States Department of Commerce National Oceanic and Atmospheric Administration*. Report, Heerbrugg 1987.

[5] H. Ingensand, *Das Rapid Precision Levelling Projekt. Die Entwicklung eines automatischen trigonometrischen Nivellementsystems mit intregiertem Dispersometer*, in Vermessungswesen und Raumordnung, Vol. 52/2+3, 1990, pages 105-114.

[6] T. Glissmann, *Zur Bestimmung des Refraktionswinkels über die Dispersion des Lichtes mittels positionsempfindlicher Photodioden*, Wissenschaftliche Arbeiten der Lehrstühle für Geodäsie, Photogrammetrie und Kartographie an der technischen Universität Hannover, Vol. 62, 1976.

[7] G. Bahnert, *Die Bestimmung der terrestrischen Refraktion aus der Dispersion des Lichtes*, in Vermessungstechnik, Vol. 2, 1982, pages 52-55.

[8] D. C. Williams, H. Kahmen, *Two wavelength angular refraction measurement*, in Geodetic Refraction, ed. F. K. Brunner, 1984, pages 7-32.

[9] A. A. M. Saleh, *An investigation of laser wave depolarization due to atmospheric transmission.* in IEEE Journal of Quantum Electronics, Vol. QE-3, No. 11, 1967, pages 540-543.

[10] M. Born, E. Wolf, *Principles of optics, 6th edition*, Pergamon Press, 1980, 808 pages.

[11] J. C. de Munck, *The theory of dispersion applied to electro-optical distance measurement and angle measurement*, Publications on Geodesy, Vol. 3, No. 4, 1970, Netherlands Geodetic Commission.

[12] H. Moritz, *Zur Reduktion elektronisch gemessener Strecken und beobachteter Winkel wegen Refraktion*, in Zeitschrift für Vermessungswesen, Vol. 7, 1961, pages 246-252.

[13] B. Edlén, *The refractive index of the air*, in Metrologia, Vol. 2, No. 2, 1966, pages 71-80.

[14] M. T. Prilepin, *Some problems in the theory of determining geodetic refraction by dispersion method*, in Bulletin Géodésique, No. 108, 1973, pages 115-123.

[15] F. K. Brunner, D. C. Williams, *On the correction for humidity in two colour refraction measurement*, in Zeitschrift für Vermessungswesen, Vol. 3, 1982, pages 108-118.

[16] M. Hennes, *Entwicklung eines Messsystems zur Ermittlung von Turbulenzparametern der Atmosphäre für Anwendungen in der Geodäsie*, Dissertation DGK, Reihe C, Vol. 438, 1995.

[17] H. Ingensand, M. Hennes, B. Boeckem, *Recent concepts for refractionfree optical measurements in tunnel and shafts*, Proceedings of the FIG Symposium on Surveying of large bridge and tunnel projects, Kopenhagen, 1997, pages 181-193.

[18] J. H. Churnside, R. J. Lataitis, L. C. Huff, *A theoretical and experimental investigation into turbulence effects on the Rapid Precision Leveling System (RPLS) dispersion subsystem*, NOAA Technical Memorandum ERL WPL-168, 1989, Wave Propagation Laboratory Boulder, Colorado, 42 pages.

[19] M. Gu, F. K. Brunner, *Theory of the two frequency dispersive range correction*, in Manuscripta Geodaetica, Vol. 15, 1990, pages 357-361.

[20] W. Huebner, *Zur Ausnutzung der Dispersion für die elektromagnetische Streckenmessung*, Dissertation DGK, Reihe C, Vol. 310, 1985.

[21] S. Nakamura, G. Fasol, *The blue laser diode, GaN based light emitters and lasers*, Springer Verlag, 1997, 344 pages.

[22] D. Fluck, *Ion-implanted $KNbO_3$ waveguides for blue-light second-harmonic generation*, Dissertation, ETH No. 11225, 1995.

[23] F. K. Brunner, *Atmospheric turbulence: The limiting factor to geodetic precision*, Aust. J. Geod. Photo. Surv., No. 31, 1979, pages 51-64.

[24] W. Schwarz, *Hochpräzise Aligniersysteme*, XI. Internationaler Kurs für Ingenieurvermessung, eds. H. J. Matthias, A. Gruen, Zurich, 1992, Vol. 1, pages II 15/1-12.

[25] W. Schwarz, *Vermessungsverfahren im Maschinen- und Anlagenbau*, Verlag Konrad Wittwer, 1995, 336 pages.

[26] B. F. Gaechter, A. M. J. Huiser, *Vermessungsgerät mit Mitteln zur Kompensation von Turbulenzeinflüssen*, German Patent, DE 3730093 C2, 1990, 8 pages.